

Open-Set Classification in a Few-shot Setting

Sayak Nag, Dripta S. Raychaudhuri, Sujoy Paul, and Amit K. Roy-Chowdhury, *Fellow, IEEE*

Abstract—In many applications, we have only a few samples of each class from which to learn to categorize them (few-shot classification). In these settings, it is very challenging to identify samples that do not lie in any of the known categories (open-set classification). The challenge of learning a good abstraction for a class with very few samples makes it extremely difficult to detect samples from the unseen categories; consequently, open-set recognition has received minimal attention in the few-shot setting. However, it is very critical in many applications like environmental monitoring where the number of labeled examples for each class is limited, while the number of classes can be very large. Most open-set few-shot classification methods consider uniform probability for open class samples, but this approach is often inaccurate, especially for fine-grained categorization. Instead, we propose a novel exemplar reconstruction based meta-learning strategy for jointly detecting open class samples, as well as, categorizing samples from seen classes via metric based classification. The exemplars, which act as representatives of a class, can either be provided in the training dataset or estimated in the feature domain. Our framework, named Reconstructing Exemplar based Few-shot Open-set Classifier (ReFOCS), has been tested on a wide variety of datasets and shown to outperform multiple state-of-the-art methods.

Index Terms—Few-Shot Learning, Open-Set Recognition, Out-of-distribution detection, Meta-learning

1 INTRODUCTION

Deep neural networks have achieved excellent performance on a wide variety of visual tasks [1], [2], [3]. However, the majority of this success has been realized under the closed-set scenario, where the training datasets are assumed to include all classes that appear during inference. Real-world applications, on the other hand, often entail acute difficulty in obtaining samples which exhaust all possible semantic categories [4]. This inherent open-ended nature of the visual world restricts the wide-scale applicability of deep models, and machine learning models in general. Thus, it is more realistic to consider an *open-set* scenario [5], where the predictive model can additionally recognise *out-of-distribution samples* (not belonging to any of the seen categories), instead of falsely predicting one of the training categories.

Notable approaches for open-set recognition involve adversarial training [6] to reject adversarial samples which are too hard to classify, inducing self-awareness in CNNs [7] to reject out-of-distribution samples, and using extreme value statistics to re-calibrate classification scores of samples from novel classes [8]. All of these approaches require large amounts of labeled data per category for the seen classes. On the contrary, humans can easily grasp new concepts with very limited supervision and simultaneously perceive the occurrence of unforeseen abnormalities. Aiming to emulate this, we seek to perform open-set recognition in the *few-shot learning* scenario, which has been largely ignored in the literature. A visual description of the problem setting is shown in Fig. 1.

The challenge in few-shot open-set recognition stems from the limited availability of samples for in-distribution classes. This complicates learning a good abstraction of the provided categories to comprehensively distinguish between low-likelihood in-distribution samples and actual out-of-distribution samples. Recently, Liu et. al. [9] attempt this task using Prototypical Networks in a meta-learning setup [10], [11], [12]. Their approach maximizes the entropy over the

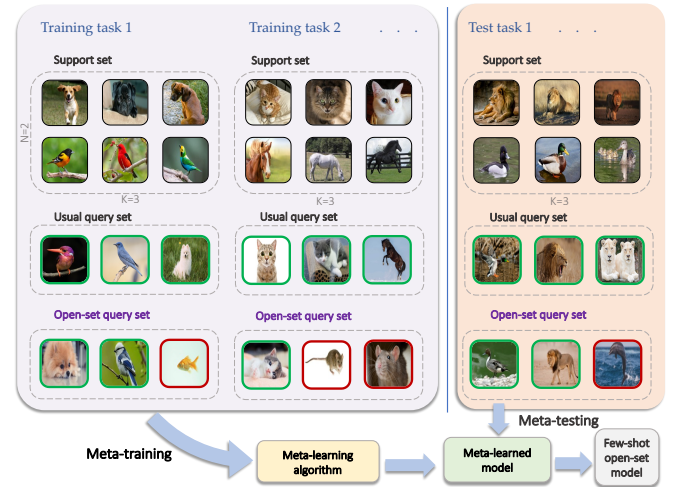


Fig. 1: **Problem setup.** We formulate few-shot open-set recognition as a meta-learning problem where training proceeds in an episodic manner. In contrast to the usual setup, where the support and query sets share the same categories, we consider the more challenging open-set scenario where the query set can contain samples from classes not seen in the support (highlighted in red).

predicted softmax scores of samples from open classes in an attempt to maximize model confusion for such unseen categories. Thus, out-of-distribution samples are desired to have a uniform predictive distribution. Unfortunately, this assumption does not hold in practice: the sensitivity of deep CNNs to minor perturbations in the input [13], in addition to the softmax function being a smooth variant of the indicator function, make them prone to producing high confidence false predictions for out-of-distribution samples [7]. This is further explained in Fig. 3.





To rectify this phenomenon, we propose a different approach to detecting out-of-distribution samples in the



Fig. 2: **Canonical Exemplars of real images.** Examples of real-world images of symbolic data such as traffic signs and brand logos (left column) along with their corresponding class-specific exemplar images (right column). These exemplars are readily available for such symbols and lie on a canonical domain devoid of perturbations of the real images.

few-shot setting which utilizes *reconstruction* as an auxiliary task. Auto-associative networks [14] use a similar concept, with the underlying idea being auto-encoders trained on “normal” data will be able to reconstruct samples from the same distribution but will fail to do so for out-of-distribution instances. However, naively applying reconstruction fails in the few-shot setting due to overfitting. Inspired by [15], we propose using reconstruction of *class-specific exemplars*, instead of self-reconstruction, to flag out-of-distribution samples. Such exemplars act as ideograms to effectively encode the semantic information of the class it belongs to. Consequently, they serve to anchor the representations of in-distribution classes when access to large number of samples is restricted. Examples of exemplar images corresponding to real-world graphical symbols, such as, traffic signs and brand logos are shown in Fig. 2. In cases where exemplars are not readily available, we provide a simple scheme to estimate them from the few-shot data in the *embedding space*, without any changes to the algorithmic formulation.

Building on this idea of reconstruction, we propose a new meta-learning strategy to tackle the few-shot open-set recognition task. In the meta-training phase, we use episodes sampled from a base set, with each episode simulating a token few-shot open-set task. Specifically, each episode is created by randomly selecting a set of classes and populating a support set with limited samples belonging to those classes. A query set is created in a similar fashion, but contains

				
Bird	0.96	0.02	0.11	0.14
Dog	0.02	0.97	0.03	0.82
Truck	0.02	0.01	0.86	0.04

■ In-distribution ■ Out-of-distribution

Fig. 3: **Assuming uniform predictive distribution for outliers.** Out-of-distribution samples can be correlated to in-distribution classes by varying amounts. In this figure, we train a classifier for three in-distribution classes: dog, bird and truck (corresponding samples highlighted in green). The out-of-distribution sample - a cat - shares highly similar visual characteristics to a dog, as evidenced by the prediction. This suggests that desiring outliers to have a uniform predictive distribution, as suggested in [9], is often inaccurate.

samples from classes both seen in the support set and beyond (see Fig. 1). These episodes are subsequently used to train our framework: Reconstructing Exemplar based Few-shot Open-set ClaSsifer (**ReFOCS**). Given an episode, ReFOCS projects these samples to a low-dimensional embedding space to perform a metric-based classification over the support classes. Simultaneously, a variational model is used to reconstruct the class exemplars (image or feature) to compute the reconstruction error. The class scores, in addition to the reconstruction error are then utilized to recognize the probability of the sample being out-of-distribution.

Main Contributions

Our primary contributions are summarized below:

- We develop a new meta-learning framework which utilizes class-specific exemplars to jointly perform few-shot classification and out-of-distribution detection.
- We introduce a novel embedding modulation scheme to make the learnt representations more robust and discriminative in the presence of scarce samples. A weighted strategy for prototype computation is also introduced for reducing intra-class bias.
- In comparison to the current state-of-the art we obtain a median increase of approximately 6% in AUROC for 5-shot experiments and around 7% for 1-shot experiments with a maximum increase of over 12%. The increased AUROC is complemented with greater or comparable classification accuracy of in-distribution samples which altogether clearly establishes our proposed approach as the new state-of-the art in few-shot open-set recognition.

2 RELATED WORKS

Few-shot learning. Few-shot learning [16], [17], [18] aims to learn representations that generalize well to novel classes with few examples. Meta-learning [19] is the one of the most common approaches for addressing this problem and it is generally grouped into one of the following categories: *gradient-based methods* [10], [20] and *metric learning methods* [11], [12]. Typical gradient based methods, such as MAML

[10] and Reptile [20], aim to learn a good representation that enables fast adaptation to a new task. On the other hand, metric-based techniques like Matching Networks [11] and Prototypical Networks [12] learn a task-specific kernel function to perform classification via a weighted nearest neighbor scheme. Our framework belongs to the latter class of methods, with the ability to work in the open-set scenario.

Out-of-distribution detection. Also known as novelty or anomaly detection, the out-of-distribution task is commonly formulated as the detection of test samples that fall outside of the data distribution used in training. Hendrycks et. al. [7] showed that softmax alone is not a good indicator of out-of-distribution probability but statistics drawn from softmax can be utilized to make assumptions of the “normalcy” of a test sample. Liang et. al. [21] re-calibrated output probabilities by applying temperature scaling and used virtual adversarial perturbations to the input to enhance the out-of-distribution capability of the model. Note that most out-of-distribution detection focuses on either detecting perturbed samples or out-of-dataset samples. In addition, these methodologies are not extendable to few shot settings.

Open-set classification. Open-set classification is slightly different from out-of-distribution detection in that it focuses on not only rejecting samples from unseen classes but also achieving proper classification on the seen categories. This is a much harder problem as opposed to just detecting perturbed/corrupted samples [9]. Recently, Bendale et. al. [8] introduced OpenMax which uses extreme value statistics to re-calibrate the softmax scores of samples from unseen classes. G-OpenMax [22] combines OpenMax with a generative model to synthesize the distribution of all unseen classes. Recently, counterfactual image generation [23] has been proposed to generate hard samples in an effort to build a more robust model. Note that all these methods are in a fully supervised learning setting and are not directly applicable to few-shot learning. Liu et. al. [9] utilize meta-learning to tackle this problem. The proposed framework, titled PEELER, builds on top of prototypical networks [12] and uses softmax scores to detect unseen categories, via maximizing the entropy for the unseen samples while training. Unlike the prior works used in large scale setting [8], [14], [23], PEELER does not try to learn the class cluster of all open classes by clubbing them as a single unseen class, but instead learns the cluster of the seen classes and detects unseen class samples if they do not fall in any of those clusters.

3 METHODOLOGY

In this section, we present our framework for open-set few-shot classification. We first provide a definition of the problem, followed by a brief overall methodology, and then present a detailed description of our framework.

Problem setting

Consider the standard few-shot learning setting, where we have access to a support set of labeled examples $\mathbb{S} = \{S_1, \dots, S_N\}$. Each $S_c = \{\mathbf{x}_i\}_{i=1}^K$ denotes a set of K examples belonging to the class y_c , for N -way K -shot recognition. We make two changes to this setup. First, we

assume the existence of class-specific exemplar images \mathbf{t}_c for each \mathbb{S}_c ; in case exemplars are not present, we estimate a class-specific exemplar for all the categories. Second, the query set \mathbb{Q} is comprised of both in-distribution and out-of-distribution samples w.r.t \mathbb{S} , i.e., $\mathbb{Q} = \mathbb{Q}_{in} \cup \mathbb{Q}_{out}$. In-distribution samples belong to classes seen in the support set while out-of-distribution samples belong to unseen classes. The goal is to detect the samples in \mathbb{Q}_{out} as out-of-distribution, while correctly classifying the samples in \mathbb{Q}_{in} .

In order to develop a strong prior for few-shot learning, we utilize a base training set of labeled samples $\mathcal{B} = \{(\mathcal{X}_c, \mathcal{Y}_c)\}_{c=1}^M$ to train our framework, where M is the set of all classes in \mathcal{B} , $\mathcal{X}_c = \{\mathbf{x}_1, \dots, \mathbf{x}_{|\mathcal{X}_c|}\}$ is the set of images in class c and \mathcal{Y}_c denotes the label. If class-specific exemplars \mathbf{t}_c are provided, we add them to \mathcal{B} to obtain $\hat{\mathcal{B}} = \{(\mathcal{X}_c, \mathcal{Y}_c, \mathbf{t}_c)\}_{c=1}^M$, otherwise we first estimate \mathbf{t}_c from \mathcal{B} as shown in section 3.5 and then add them to \mathcal{B} to get $\hat{\mathcal{B}}$ in a similar fashion. Like prior work [11], [12] a set of training tasks or episodes $\{\mathcal{T}_1, \mathcal{T}_2, \dots\}$ are sampled from $\hat{\mathcal{B}}$ to conduct meta-training of the model. Each episode \mathcal{T} consists of a support set \mathbb{S} of N randomly sampled classes, containing K randomly chosen samples from each class, along with a query set \mathbb{Q} constructed in a similar fashion. In order to simulate the presence of out-of-distribution samples, we follow the strategy outlined in [9] and augment the query set with samples from classes *absent* in the support.

Overall framework

A pictorial description of our framework is shown in Fig. 4. Given a sample \mathbf{x} , we first use variational inference to reconstruct the possible exemplar \mathbf{t} associated with the ground-truth class of \mathbf{x} and simultaneously obtain a latent representation of the same sample. This embedding is used to obtain a classification score, similar to [11], [24], while the reconstructed exemplar is used as a proxy for the out-of-distribution detection task. Specifically, if $\mathbf{x} \in \mathbb{Q}_{out}$, we hypothesize that the reconstruction will fail for all the exemplars of the support classes. Based on this hypothesis, the latent representation, classification scores, and the reconstruction errors (with respect to support exemplars) are subsequently fed into a binary classifier to predict the probability of the sample \mathbf{x} being out-of-distribution.

3.1 Exemplar reconstruction from real images

Since the class-specific exemplars \mathbf{t} form a compact representation of the real world images belonging to that class, we hypothesize that the ability to reconstruct any exemplar belonging to in-distribution classes correlates positively with the sample being an in-distribution one. Inspired by [15], we use a Variational Auto-Encoder (VAE) [25] for the purpose of such reconstruction. The choice of VAE is motivated by its robustness to outliers and better generalization to unseen data, as shown in [26]. This is ideal for the image-to-exemplar translation task where the exemplars lie on a canonical domain devoid of the perturbations in real images.

Given an input sample \mathbf{x} , its exemplar reconstruction of \mathbf{t} is carried out by maximizing the variational lower bound of the likelihood $p(\mathbf{t})$ [15] as follows,

$$\log p(\mathbf{t}) \geq \mathbb{E}_{q_\phi(\mathbf{z}|\mathbf{x})}[\log p_\theta(\mathbf{t}|\mathbf{z})] - D_{KL}[q_\phi(\mathbf{z}|\mathbf{x})||p(\mathbf{z})] \quad (1)$$

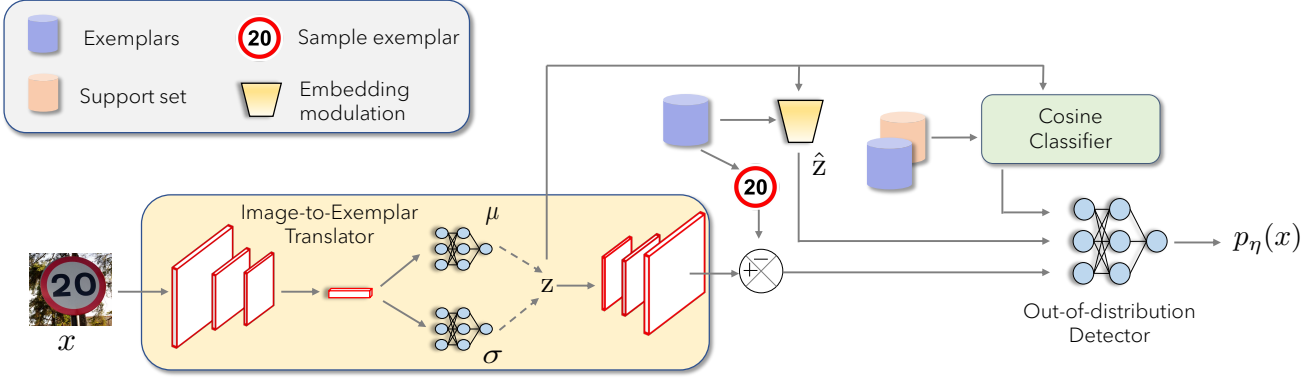


Fig. 4: **Overview of framework.** Given a query sample x , a latent representation z is derived by sampling from the variational posterior. This embedding is further enhanced via a modulation process to get \hat{z} . The latent embedding and its enhanced version are used for classifying the sample into one of the few-shot classes and also to predict whether it is an out-of-distribution instance by utilizing exemplar reconstruction.

where $D_{KL}[\cdot]$ is the Kullback-Leibler (KL) divergence and $q_\phi(\mathbf{z}|\mathbf{x})$ denotes the variational distribution introduced to approximate the intractable posterior. Note that this is different from a vanilla VAE [25], which is derived by maximizing the log-likelihood of the input data \mathbf{x} . A differentiable version of the lower bound is derived by assuming the latent variable \mathbf{z} to be Gaussian in nature, sampled from the prior $q_\phi(\mathbf{z}|\mathbf{x})$. The empirical loss to be minimized is given as follows,

$$\mathcal{L}_{VAE} = \frac{1}{K_e} \sum_{i=1}^{K_e} -\log p_\theta(\mathbf{t}_i|\mathbf{z}_i) + D_{KL}[q_\phi(\mathbf{z}|\mathbf{x})||p(\mathbf{z})] \quad (2)$$

where K_e is the number of samples in one episode, i.e., $K_e = |\mathbb{S} \cup \mathbb{Q}_{in}|$. Since $\mathbf{z} \sim q_\phi(\mathbf{z}|\mathbf{x})$ is non-differentiable, the re-parameterization trick is applied via the decoder network [25] such that $\mathbf{z} = \mu + \sigma \odot \epsilon$, where $\epsilon \sim \mathcal{N}(0, \mathbf{I})$ and \odot is the Hadamard product.

The first term in Eq. 2 is the reconstruction loss which affects the mapping of the real images to their class specific exemplars, while the second term acts as a distribution regularization, enforcing the latent variable \mathbf{z} to follow the chosen prior. Although binary cross entropy (BCE) is the common choice for the reconstruction loss in VAE, other losses such as ℓ_1 or ℓ_2 norm can also be used. The choice of reconstruction loss used in our experiments can be found in Section 4.

3.2 Few-shot classification

The latent representation of a query sample \mathbf{z}_q , obtained from the encoder in the previous section, is used for computing the classification scores. We use the cosine metric to compute a relation score between the query sample and the support set \mathbb{S} . Specifically, the relation score is obtained by computing the cosine similarity between \mathbf{z}_q and the set of prototypes or centroids, $\{\Omega_c\}_{c=1}^N$ for each class $c \in \mathbb{S}$ (Fig. 4). The classification score for \mathbf{x}_q is obtained by performing a softmax operation on these relation scores. In contrast to prior works [9], [12], the class specific prototype Ω_c is obtained by a weighted mean of the support samples instead of a simple mean. Note that these prototypes are different from the class specific exemplars \mathbf{t} .

Prototype computation

Given the support set, the prototypes for each class c are calculated as follows,

$$\Omega_c = \sum_{k=1}^K \omega_k \cdot \mathbf{z}_k^c \quad (3)$$

\mathbf{z}_k^c denotes the latent representation of $\mathbf{x}^k \in \mathbb{S}_c$, while ω_k is the weight assigned to \mathbf{z}_k^c based on how close it is from the embedding of the exemplar belonging to the c^{th} class, \mathbf{z}_t^c ,

$$\omega_k = \frac{e^{\cos(\mathbf{z}_k^c, \mathbf{z}_t^c)}}{\sum_{k=1}^K e^{\cos(\mathbf{z}_k^c, \mathbf{z}_t^c)}} \quad (4)$$

We use these weights in an effort to control the phenomena of *intra-class bias* [27], i.e., the difference between the true expected prototype and the Monte-Carlo estimated value. As explained earlier, each of the exemplars are an effective ideogram which provide a good abstraction of their respective classes. Thus the image-to-exemplar translation learned by the VAE leads to a feature space where the embedding of the real images cluster around that of their corresponding exemplars. This makes the exemplars good approximation of the true prototype and we leverage this via the weights ω_k to alleviate the intra-class bias.

Classification

After computing the prototypes, we predict the classification scores for the query sample x_q as follows,

$$p_\phi(y = c|\mathbf{x}_q) = \frac{e^{\tau \cdot \cos(\mathbf{z}_q, \Omega_c)}}{\sum_{c'} e^{\tau \cdot \cos(\mathbf{z}_q, \Omega_{c'})}} \quad (5)$$

where τ is a learnable temperature parameter to scale the logits computed by cosine similarity [24], [28]. Learning proceeds by minimizing a cross-entropy loss over the in-distribution classes as follows:

$$\mathcal{L}_{CE} = -\frac{1}{|\mathbb{Q}_{in}|} \sum_{i=1}^{|\mathbb{Q}_{in}|} \sum_{c=1}^N \mathbb{1}\{y_i = c\} \log p_\phi(y = c|\mathbf{x}_{q,i}) \quad (6)$$

where y_i represents the true class of the query sample.

3.3 Out of distribution detection

Unlike prior work we do not rely solely on the classification score to detect out-of-distribution query samples. Instead, ReFOCS flags query samples by leveraging the output a multi-layer perceptron classifier. This binary classifier takes into account three sources of information for scoring the openness of a query sample. These three different sources are: (i) the class probability \mathbf{p}_ϕ as predicted in Eq. 5, (ii) a modulated version of the latent representation \mathbf{z} (described below), and (iii) the set of reconstruction errors with respect to the support set exemplars, $\mathbf{D} = \left[\|\hat{\mathbf{t}} - \mathbf{t}_1\|_F^2, \dots, \|\hat{\mathbf{t}} - \mathbf{t}_N\|_F^2 \right]$. \mathbf{D} indicates how far the reconstructed exemplar $\hat{\mathbf{t}}$ deviates from the actual exemplar $\mathbf{t} \in \mathbb{S}$. Intuitively, for out-of-distribution samples all the entries of \mathbf{D} will be very high, while for in-distribution samples, at least one of them will be very small.

Embedding Modulation

At a fine-grained level many of the out-of-distribution classes can have very similar visual features with some of the in-distribution classes (Fig 3. This issue becomes more relevant for the few-shot setting since the model does not have access to large amounts of samples from the in-distribution classes for generalization. Therefore, it is of paramount importance to obtain an embedding space that is discriminative enough to provide good segregation between in-distribution and out-of-distribution classes given only a handful of samples from the in-distribution classes. This, in turn, will help the classifier in better detecting the out-of-distribution samples. While the latent embedding obtained from the VAE does have good discriminative properties, we introduce an additional modulation step which can enhance it even further. We do this by scaling the embedding of a query sample \mathbf{z}_q with a scalar $\kappa > 0$ as shown below,

$$\hat{\mathbf{z}}_q = \frac{\mathbf{z}_q}{\kappa}, \text{ where } \kappa = \min_{c \in \mathbb{S}} \|\mathbf{z}_q - \Omega_c\|_1 \quad (7)$$

where $c \in \{1, \dots, N\}$ represents the classes in the support and Ω_c is the prototype corresponding to the c^{th} class. κ is a modulation factor which measures how close a query sample is to any of the in-distribution [29]. Since the samples belonging to a specific class tend to cluster around the embedding of its exemplar and therefore the prototype, out-of-distribution samples will have a higher value for κ compared to in-distribution samples, thereby, amplifying the embedding value for the in-distribution queries while scaling it down for out-of-distribution queries.

Therefore, the final input to the classifier is the concatenated vector $[\mathbf{p}_\phi, \hat{\mathbf{z}}_q, \mathbf{D}]$. Training proceeds by minimizing binary cross-entropy loss as follows,

$$\mathcal{L}_{BCE} = -\frac{1}{|\mathbb{Q}|} \sum_{i=1}^{|\mathbb{Q}|} y_{\eta,i} \log p_{\eta,i} + (1 - y_{\eta,i}) \log(1 - p_{\eta,i}) \quad (8)$$

where y_η is equal to 0 or 1 depending on whether $x_q \in \mathbb{Q}_{in}$ or $x_q \in \mathbb{Q}_{out}$ respectively.

3.4 Training

The parameters of the Encoder (ϕ), Decoder (θ) and the out-of-distribution classifier (η) are jointly meta-trained by optimizing over the aggregate loss \mathcal{L} ,

$$\mathcal{L} = \lambda_1 \mathcal{L}_{VAE} + \lambda_2 \mathcal{L}_{CE} + \lambda_3 \mathcal{L}_{BCE} \quad (9)$$

where λ_1, λ_2 and λ_3 are hyper-parameters, choices of which is discussed in Section 4.

3.5 Estimation of exemplars

For images of graphical symbols there exists well-defined exemplars which provide a good abstraction of its corresponding class. However, such class-specific exemplars need not be always provided for all natural images. In that case, we first perform non-episodic training of the VAE encoder, f_ϕ on the entire base set \mathcal{B} . Following this, the category wise samples in \mathcal{B} are passed through the pre-trained encoder and their corresponding feature representations, $f_\phi(\mathbf{x}_c)$ are extracted from the penultimate layer of the encoder. The class-specific exemplar is then computed as follows,

$$\mathbf{t}_c = \min_{c \in \mathcal{B}} \|f_\phi(\mathbf{x}_c) - \Psi_c\|_2 \quad (10)$$

where, $\Psi_c = \frac{1}{|\mathcal{B}_c|} \sum_{c \in \mathcal{B}} f_\phi(\mathbf{x}_c)$ is the centroid of the c^{th} training class in the feature space.

For test episodes we simply compute a centroid for the support samples using the representation from the meta-trained encoder and choose the support sample closest to this centroid as the exemplar for that particular test episode.

4 EXPERIMENTS

In this section we provide comprehensive experiments over several data sets to prove the efficacy of our framework, ReFOCS, for few-shot open-set classification. We compare the performance of ReFOCS with the current state-of-the-art methods that rely on the regularization/re-calibration of softmax scores for the detection of out-of-distribution samples. The results clearly establishes our method as the new state-of-the-art for few-shot open-set classification.

Datasets

We use six datasets to setup three different types of open-set recognition tasks: (i) *traffic sign recognition*, for which we use the GTSRB [30] and TT100K [31] datasets, (ii) *brand logo recognition*, for which we use BelgaLogos [32], [33], FlickrLogos-32 [34] and TopLogo-10 [35], and (iii) *natural image classification* on the *miniImageNet* dataset, using the same splits as introduced by Vinyals et.al. [11]. It must be noted that all the traffic sign and logo datasets are provided with well-defined canonical exemplars for each of the classes. Therefore, for these datasets we utilize the given exemplar for the auxiliary reconstruction task where else, for *miniImageNet* which is not provided with any well-defined exemplars, we utilize the strategy explained in section 3.5 to estimate the exemplars for the base training set, as well as, the test episodes. The datasets are configured by varying the meta-training and meta-testing datasets to obtain five few-shot scenarios as shown in Tables 2 3 and 4. Some of these scenarios involve cross-dataset experimentation which is more challenging compared to using splits from the same dataset and better mimics real-world scenarios where training and test data can have significant domain shifts [36]. For the traffic sign and natural image datasets, we evaluate our model on both the 5-way 5-shot and the

DATASETS	GTSRB→GTSRB		GTSRB→TT100K		Belga→Flickr32	Belga→Toplogos	miniImageNet→miniImageNet	
EXPERIMENT	5-way 5-shot	5-way 1-shot	5-way 5-shot	5-way 1-shot	5-way 1-shot	5-way 1-shot	5-way 1-shot	5-way 1-shot
$\mathbf{K}_{Q_{in}}^c$	10	10	10	10	1	1	15	15
$\mathbf{K}_{Q_{out}}$	50	50	50	50	5	5	75	75
\mathbf{E}_{train}	20	20	20	20	50	50	50	50
\mathbf{E}_{test}	800	800	800	800	1700	400	600	600

TABLE 1: **Sampling strategy.** Episodic sampling strategy for each of the few-shot experiments.

5-way 1-shot tasks, while for the logo classification task, we show results only on the 5-way 1-shot scenario. This is due to BelgaLogos and Toplogos having multiple classes with less than 5 samples. More details on these datasets and splits can be found in the supplementary material.

Sampling Strategies

The episodic sampling strategies for all the few-shot experiments are shown in Table 1. For an N-way K shot problem each episode \mathcal{T} has $\mathbf{K}_{Q_{in}}^c$ number of in-distribution queries sampled from each support class $c \in \{1, \dots, N\}$. Therefore, the total number in-distribution query samples per episode $\mathbf{K}_{Q_{in}} = \sum_{c=1}^N \mathbf{K}_{Q_{in}}^c$. Along with the in-distribution samples, the query set of each episode is also augmented with $\mathbf{K}_{Q_{out}}$ samples which do not belong to any of the support classes i.e. out-of-distribution. Hence, the total number of samples \mathbf{K}_e , in each episode is given as, $\mathbf{K}_e = \mathbf{K} + \mathbf{K}_{Q_{in}} + \mathbf{K}_{Q_{out}}$ where, $\mathbf{K} = |\mathcal{S}|$. The model is trained on \mathbf{E}_{train} number of episodes each epoch and meta-tested on \mathbf{E}_{test} number of test episodes.

Implementation

For the traffic sign and logo classification experiments, the VAE architecture is adapted from [15], while for the natural image classification task, we design the VAE using a ResNet-18 [37] encoder and an inverted ResNet-18 as the decoder. The novelty module is implemented as a multi-layered perceptron with two hidden layers of 200 and 100 nodes respectively. For a fair comparison, the encoder network is kept the same for all competing methods. Similar to [15], the embedding size is set to 300 for the traffic sign and logo datasets, while the ResNet-18 encoder is used to obtain a 512 dimensional feature representation for the natural image classification task. The Adam optimizer [38] is used for all the experiments. For all the traffic sign and brand logo recognition experiments the values of the loss function hyperparameters, λ_1, λ_2 and λ_3 , are set to $10^{-4}, 10$ and 10 respectively. For the natural image classification task on miniImageNet λ_1, λ_2 and λ_3 , are set to $10^{-4}, 1$ and 10 respectively. Additional ablation study on the choice of these hyperparameters is provided in the supplementary materials.

Baselines

We compare ReFOCS against Prototypical Networks (ProtoNet) [12], which is implemented with the euclidean distance metric, and PEELER [9] which uses the Mahalanobis distance metric. While not originally designed for open-set classification, ProtoNet provides a lower bound on performance for comparison, and on the other hand, PEELER is the sole method, to the best of our knowledge, that addresses few-shot open-set classification. We also compare

against OpenMax [8], which was originally proposed for out-of-distribution detection in the fully supervised setting. Since OpenMax re-calibrates the softmax score to reject out-of-distribution samples, we implement it over the standard prototypical network in order to adapt it for the few-shot setting, and henceforth we denote this baseline as Proto+OM.

Evaluation Metrics

To quantify the closed-set classification performance we compute the accuracy over in-distribution queries, and utilize the Area Under the Receiver Operating Characteristic curve (AUROC) to quantify the model’s performance in detecting the open classes. For all our evaluations, we split the query set equally among in-distribution and out-of-distribution samples.

4.1 Traffic Sign Recognition

The performance of ReFOCS on the two traffic sign recognition tasks, GTSRB→GTSRB and GTSRB→TT100K, is shown in Table 2. GTSRB and TT100K have a total of 43 and 36 classes respectively. For GTSRB→GTSRB, 22 classes are used for meta training, and the remaining 21 are used for meta testing. For GTSRB→TT100K, all classes of GTSRB are used for training with testing being done on all the classes of TT100K. In both experiments all images are resized to 64×64 . For both cases, the framework was meta-trained for 20000 episodes and the standard BCE criterion was used for computing the VAE reconstruction loss. A learning rate of 10^{-4} is used for both experiments. As shown in Table 2, ReFOCS outperforms all baselines in detecting the out-of-distribution samples. On average, the AUROC score achieved by ReFOCS is **10.4%** higher than the competing methods. The problem of using softmax values as an open-set indicator can be clearly seen in the lower AUROC values of ProtoNet, Proto+OM and PEELER. The issue is more pronounced for ProtoNet, since, unlike the PEELER and Proto+OM, ProtoNet does not explicitly regularize the probability scores of out-of-distribution samples which results in even more high-confidence false predictions. The efficacy of our proposed prototype computation (Eq. 4) is also evidenced by the higher classification accuracy - **1.22%** on average - in comparison to the baselines. This shows that the weighted prototype computation leads to more *unbiased* prototypes as opposed to those computed baselines. Some sample exemplar reconstructions are provided in Fig 5.

4.2 Brand Logo Recognition

The brand logo datasets consist of everyday images of commercial brand logos. In both of the two few-shot tasks, Belga→Flickr32, and Belga→Toplogos, the Belga dataset,

MODEL	METRIC	GTSRB→GTSRB		GTSRB→TT100K	
		Acc. (%)	AUROC(%)	Acc. (%)	AUROC (%)
5-way 5-shot					
PROTONET [12]	Euclidean	91.79 ± 0.44	70.74 ± 0.79	80.51 ± 0.78	62.10 ± 0.76
PROTO+OM [8]	Euclidean	91.92 ± 0.43	86.67 ± 0.48	64.40 ± 0.78	68.80 ± 0.66
PEELER [9]	Mahalanobis	93.87 ± 0.37	90.99 ± 0.44	79.04 ± 0.79	73.25 ± 0.81
REFOCS(Ours)	Cosine	94.17 ± 0.38	94.83 ± 0.35	83.36 ± 0.76	85.25 ± 0.56
5-way 1-shot					
PROTONET [12]	Euclidean	82.31 ± 0.75	61.52 ± 0.90	69.82 ± 0.87	56.02 ± 0.83
PROTO+OM [8]	Euclidean	82.46 ± 0.70	81.43 ± 0.65	55.10 ± 0.80	67.79 ± 0.66
PEELER [9]	Mahalanobis	82.86 ± 0.77	79.56 ± 0.85	73.47 ± 0.88	69.68 ± 0.88
REFOCS (Ours)	Cosine	86.21 ± 0.78	93.02 ± 0.45	71.45 ± 0.87	81.98 ± 0.59

TABLE 2: **5-way 5-shot and 5-way 1-shot results of traffic sign recognition.** For both traffic sign datasets GTSRB→GTSRB and GTSRB→TT100K, 800 test episodes were evaluated and the average performance is reported along with their 95% confidence levels.

MODEL	METRIC	BELGA→TOPLOGOS		BELGA→FLICKR32	
		Acc. (%)	AUROC(%)	Acc. (%)	AUROC (%)
PROTONET [12]	Euclidean	59.50 ± 0.99	58.69 ± 0.94	38.08 ± 2.10	53.18 ± 1.97
PROTO+OM [8]	Euclidean	59.60 ± 1.01	61.00 ± 1.02	38.20 ± 1.95	56.40 ± 1.92
PEELER [9]	Mahalanobis	62.93 ± 1.03	66.40 ± 0.86	39.55 ± 2.05	56.25 ± 1.94
REFOCS (Ours)	Cosine	66.29 ± 1.02	72.98 ± 0.83	42.30 ± 2.15	58.39 ± 1.97

TABLE 3: **5-way 1-shot results of brand logo recognition.** For **Belga→Flickr32**, 1700 test episodes were evaluated and for **Belga→Toplogos**, 400 test episodes were evaluated and their average closed-set Accuracy and open-set AUROC are reported with 95% confidence intervals.

which has 37 classes, is used for meta-training our framework. Flickr32 and Toplogos each have 32 and 11 classes respectively. Since some of the classes have as low as 2 samples, we restrict our experiments to the 5-way 1-shot scenario (Table 3). In both cases all images are resized to 64×64 . We meta-train our framework for 50000 episodes for both recognition experiments, using a learning rate of 10^{-4} . From the results shown in Table 3, it is evident that ReFOCS achieves significant gains in both accuracy and AUROC, outperforming PEELER [9] by an average of 4.28% in AUROC and 3.05% in classification accuracy. This clearly highlights the superiority of our approach for few-shot open-set recognition. The in-distribution classification accuracy, although better than the competing baselines, is lower in comparison to the traffic sign datasets, which is due to the lower quality of the training set, as pointed out in [15]. In addition, there is a significant domain gap between the images and exemplars of Belga and that of Toplogos, which makes it even more difficult to achieve good classification accuracy.

4.3 Natural Image Classification

The *miniImageNet* dataset, introduced in [11], is a benchmark dataset used for evaluating the performance of models for

few-shot natural image classification. This dataset has a total of 100 classes and as per the splits introduced in [11] 64 classes are used for training, 16 for validation and the remaining 20 for testing. The images are resized to the standard resolution of 84×84 [11]. As explained previously, this dataset does not have any categorical exemplars - we use the strategy explained in section 3.5 to estimate the category-specific exemplars for our experiments. For both the 5-way 5-shot and 5-way 1-shot scenarios, ReFOCS is meta-trained with 50000 episodes. It must be noted that the estimated exemplars are not on a canonical domain unlike those of the traffic sign and brand logo datasets. This makes the image-to-image translation for exemplar reconstruction even more challenging, specifically due to the presence of varying lighting and color contrasts in the real domain. Consequently, the standard BCE reconstruction loss is not able to compensate for these perturbations, and thus, we use the ℓ_2 norm as the reconstruction criterion, which leads to a marked improvement in the results. For this dataset we use an initial learning rate of 10^{-3} which is dropped by a factor of 10 every 20000 episodes. From Table 4 we can clearly see that ReFOCS outperforms the baselines especially for the open sample detection as evidenced by the higher AUROC scores. Many of the *miniImageNet* objects have fine-grained visual

MODEL	METRIC	<i>miniImageNet</i> → <i>miniImageNet</i>			
		5-way 5-shot		5-way 1-shot	
		Acc.(%)	AUROC(%)	Acc.(%)	AUROC(%)
PROTONET [12]	Euclidean	78.11 ± 1.22	58.67 ± 0.45	55.18 ± 1.36	56.51 ± 0.47
PROTO+OM [8]	Euclidean	79.01 ± 1.21	54.16 ± 0.47	55.73 ± 1.36	45.09 ± 0.39
PEELER [9]	Mahalanobis	63.60 ± 0.67	64.17 ± 0.64	48.49 ± 0.81	59.39 ± 0.77
PEELER ⁺ [9]	Mahalanobis	75.08 ± 0.72	69.85 ± 0.70	58.31 ± 0.58	61.66 ± 0.62
ReFOCS(Ours)	Cosine	79.06 ± 1.17	69.91 ± 0.51	58.33 ± 0.84	69.24 ± 0.59

TABLE 4: **5-way 5-shot and 5-way 1-shot results of natural image classification.** For the natural images the performance is averaged over 600 test episodes. PEELER⁺ denotes the corresponding results reported in [9] while PEELER, in the previous row, denotes the results obtained via the official implementation¹. All results are reported with 95% confidence levels.

EXPERIMENT	GTSRB→TT100K		BELGA→FLICKR32	
	5-way 5-shot		5-way 1-shot	
	Acc.(%)	AUROC(%)	Acc.(%)	AUROC(%)
Recons. w/ AE	81.33 ± 0.80	77.08 ± 0.79	63.13 ± 1.05	71.86 ± 0.86
No modulation	80.94 ± 0.79	78.55 ± 0.65	63.26 ± 1.03	56.69 ± 0.97
ProtoC+ND	76.92 ± 0.83	72.50 ± 0.61	61.64 ± 1.03	50.01 ± 0.99
No embedding	83.03 ± 0.75	74.33 ± 0.66	65.49 ± 1.00	67.79 ± 0.91
No clf	82.71 ± 0.74	82.85 ± 0.56	64.51 ± 1.01	71.58 ± 0.87
ReFOCS (Ours)	83.36 ± 0.76	85.25 ± 0.56	66.29 ± 1.02	72.98 ± 0.83

TABLE 5: **Ablation studies.** Recons. w/ AE refers to swapping the VAE with an Autoencoder (AE); No Modulation denotes turning off embedding modulation; No embedding/clf denote the removal of embedding/softmax scores from the input of the novelty module. ProtoC+ND refers to when we donot use exemplars for the reconstruction and consequently, remove the reconstruction errors from the input of the novelty module.

DATASET	SETTING	METRIC	ACC.	AUROC
GTSRB→TT100K	5-shot	Cosine	83.36 ± 0.76	85.25 ± 0.56
		Euclidean	78.77 ± 0.74	81.42 ± 0.51
Belga→Flickr32	1-shot	Cosine	66.2 ± 1.02	72.9 ± 0.83
		Euclidean	48.73 ± 0.99	50.61 ± 0.95
<i>miniImageNet</i>	5-shot	Cosine	79.06 ± 1.17	69.91 ± 0.51
		Euclidean	79.09 ± 1.15	52.83 ± 0.48

TABLE 6: **Choice of metric.** Effect on performance as the similarity metric is varied.

differences (eg: cats and dogs) - this makes ProtoNet, which relies on the raw softmax score, prone to misclassification of the unseen categories as one of the seen ones. This is reflected in the performance of ProtoNet as it is barely able to achieve better than random AUROC (Table 2). Unlike the prior experiments, Proto+OM fails to achieve a decent AUROC score. This is predominantly due to the failure of OpenMax to fit a Weibull distribution with just a handful of samples for each of the novel test categories during the meta-testing phase. As a result, OpenMax fails to recalibrate the ProtoNet’s logits with such a small number of support samples. Note that PEELER fails to achieve the reported performance on the *miniImageNet* experiments [9] when

results are generated by using the official implementation¹.

4.4 Ablation Studies

In this section we use two cross-dataset scenarios to perform ablation studies of different components of our framework to understand their contribution towards the final performance.

Impact of using variational encoding.

The reconstruction module of ReFOCS is designed using a VAE [15] due to its better generalization ability [26]. We highlight this by replacing the VAE and experimenting with

1. <https://github.com/BoLiu-SVCL/meta-open/>

a standard auto-encoder (AE). As shown in Table 5, the classification performance drops significantly, along with a drop in the AUROC.

Impact of embedding modulation.

The importance of the embedding modulation can be clearly seen from Table 5. The modulated embedding results in more distinct feature representations with adequate segregation between the seen and unseen classes, thereby, making it easier for the novelty module to flag unseen categories. Removing it results in a significant drop in AUROC and on the other hand it’s presence also amplifies the classification performance. This suggests that the improvement of the open class detection is complemented by improvement in seen class categorisation.

Input to the novelty module.

We feed a concatenation of the modulated embedding, classification score and ℓ_2 reconstruction errors to the novelty module. Empirically, the combination of all three gives the best results for out-of-distribution detection. We study the impact of removing the classification score or the embedding from the input and as seen from the results in Table 5, in both cases there is a drop in both the classification accuracy and the AUROC score. Additionally, we also examine the scenario when we do not use any exemplar for reconstruction, and consequently, feed in just the classification score and the raw embedding as input to the novelty module. We call this variant of ReFOCS, ProtoC+ND and as seen from Table 5 the removal of the exemplar reconstruction errors result in the biggest drop in performance - with AUROC dropping to 50% in one case (random prediction) - which again consolidates the impact of the exemplars in out-of-distribution detection.

Choice of distance metric.

Computing the logits for classification requires a distance metric to measure the similarity between the prototypes and the sample in the latent space. We experiment with both the cosine and euclidean metrics and choose the cosine distance as it leads to more a discriminative embedding space [27], [28]. This is particularly important for segregating the open class samples from the support class ones. This is validated by the results shown in Table 6, where we can see that choosing the euclidean distance metric leads to a significant drop in AUROC.

Embedding Visualization.

In Fig. 6 we compare the t-SNE [39] visualization of the embedding spaces induced by all the competing methods. We can see from Fig. 6 that, in general, ReFOCS achieves more distinct class clusters in comparison to both PEELER [9] and ProtoNet [12], with adequate segregation between seen and unseen classes.

5 CONCLUSION

In this work, we present a novel strategy for addressing few shot open-set recognition. We frame the few-shot open-set classification task as a meta learning problem similar to [9], but unlike their strategy, we do not solely rely on the softmax score as an indication of an open class. We argue that



Fig. 5: **Sample exemplar reconstructions for GTSRB→GTSRB.** Exemplar reconstructions of a few query samples from 1 test episode. (a) Class-wise exemplars provided in the support set. (b) In-distribution query samples. (c) Out-of-distribution query samples. (d) Reconstructed exemplars from the in-distribution queries. (e) Reconstructed Exemplars from the out-of-distribution queries, as hypothesized when out-of-distribution samples are fed into ReFOCS it fails to reconstruct the class-wise exemplars given in the support.

the proclivity of softmax to overfit to unseen classes makes it an unreliable choice as an open-set indicator, especially when there is a dearth of samples. Instead we propose to use a reconstruction of exemplar images as a key signal to detect out-of-distribution samples. The learned embedding which is used to classify the sample is further modulated to ensure proficient gap between the seen and unseen class

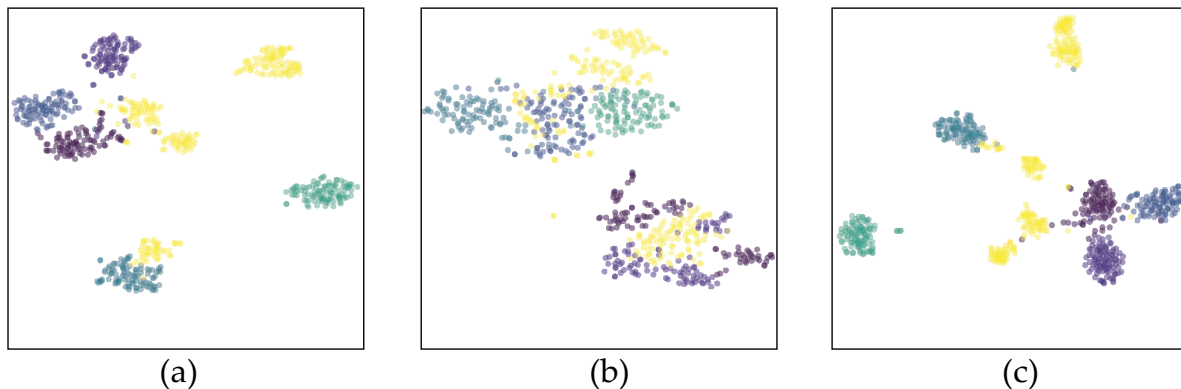


Fig. 6: **t-SNE visualization.** We project the latent space learned via (a) ProtoNet (b) PEELER (c) ReFOCS, on 5 classes of GTSRB→TT100K, on a 2D space using t-SNE. Out-of-distribution queries are in yellow

clusters in the feature space. Finally the scaled embedding, the softmax score and the quality reconstructed exemplar are jointly utilized to cognize if the sample is in-distribution or out-of-distribution. The enhanced performance of our framework is verified empirically over a wide variety of few-shot tasks and the results establish it as the new state-of-the-art. In the future, we would like to extend this approach to more cross-domain few-shot tasks, including videos.

REFERENCES

- [1] K. He, X. Zhang, S. Ren, and J. Sun, “Deep residual learning for image recognition,” in *Proceedings of the IEEE conference on computer vision and pattern recognition*, 2016, pp. 770–778.
- [2] T.-Y. Lin, P. Dollár, R. Girshick, K. He, B. Hariharan, and S. Belongie, “Feature pyramid networks for object detection,” in *Proceedings of the IEEE conference on computer vision and pattern recognition*, 2017, pp. 2117–2125.
- [3] J. Long, E. Shelhamer, and T. Darrell, “Fully convolutional networks for semantic segmentation,” in *Proceedings of the IEEE conference on computer vision and pattern recognition*, 2015, pp. 3431–3440.
- [4] Z. Liu, Z. Miao, X. Zhan, J. Wang, B. Gong, and S. X. Yu, “Large-scale long-tailed recognition in an open world,” in *IEEE Conference on Computer Vision and Pattern Recognition (CVPR)*, 2019.
- [5] C. Geng, S.-j. Huang, and S. Chen, “Recent advances in open set recognition: A survey,” *IEEE transactions on pattern analysis and machine intelligence*, 2020.
- [6] J. Lu, T. Issaranon, and D. Forsyth, “Safetynet: Detecting and rejecting adversarial examples robustly,” in *Proceedings of the IEEE International Conference on Computer Vision (ICCV)*, Oct 2017.
- [7] D. Hendrycks and K. Gimpel, “A baseline for detecting misclassified and out-of-distribution examples in neural networks,” *Proceedings of International Conference on Learning Representations*, 2017.
- [8] A. Bendale and T. E. Boulton, “Towards open set deep networks,” in *Proceedings of the IEEE Conference on Computer Vision and Pattern Recognition (CVPR)*, June 2016.
- [9] B. Liu, H. Kang, H. Li, G. Hua, and N. Vasconcelos, “Few-shot open-set recognition using meta-learning,” in *2020 IEEE/CVF Conference on Computer Vision and Pattern Recognition (CVPR)*, 2020, pp. 8795–8804.
- [10] C. Finn, P. Abbeel, and S. Levine, “Model-agnostic meta-learning for fast adaptation of deep networks,” ser. *Proceedings of Machine Learning Research*, D. Precup and Y. W. Teh, Eds., vol. 70. International Convention Centre, Sydney, Australia: PMLR, 06–11 Aug 2017, pp. 1126–1135. [Online]. Available: <http://proceedings.mlr.press/v70/finn17a.html>
- [11] O. Vinyals, C. Blundell, T. Lillicrap, K. Kavukcuoglu, and D. Wierstra, “Matching networks for one shot learning,” in *Proceedings of the 30th International Conference on Neural Information Processing Systems*, ser. NIPS’16. Red Hook, NY, USA: Curran Associates Inc., 2016, p. 3637–3645.
- [12] J. Snell, K. Swersky, and R. Zemel, “Prototypical networks for few-shot learning,” in *Proceedings of the 31st International Conference on Neural Information Processing Systems*, ser. NIPS’17. Red Hook, NY, USA: Curran Associates Inc., 2017, p. 4080–4090.
- [13] I. Goodfellow, J. Shlens, and C. Szegedy, “Explaining and harnessing adversarial examples,” in *International Conference on Learning Representations*, 2015. [Online]. Available: <http://arxiv.org/abs/1412.6572>
- [14] M. A. F. Pimentel, D. A. Clifton, L. Clifton, and L. Tarassenko, “Review: A review of novelty detection,” vol. 99, p. 215–249, Jun. 2014. [Online]. Available: <https://doi.org/10.1016/j.sigpro.2013.12.026>
- [15] J. Kim, T.-H. Oh, S. Lee, F. Pan, and I. S. Kweon, “Variational prototyping-encoder: One-shot learning with prototypical images,” in *Proceedings of the IEEE Conference on Computer Vision and Pattern Recognition*, 2019, pp. 9462–9470.
- [16] M. Rohrbach, S. Ebert, and B. Schiele, “Transfer learning in a transductive setting,” in *Advances in neural information processing systems*, 2013, pp. 46–54.
- [17] D. S. Raychaudhuri and A. K. Roy-Chowdhury, “Exploiting temporal coherence for self-supervised one-shot video re-identification,” *arXiv preprint arXiv:2007.11064*, 2020.
- [18] J. Guan, Z. Lu, T. Xiang, A. Li, A. Zhao, and J.-R. Wen, “Zero and few shot learning with semantic feature synthesis and competitive learning,” *IEEE transactions on pattern analysis and machine intelligence*, vol. 43, no. 7, pp. 2510–2523, 2020.
- [19] T. Hospedales, A. Antoniou, P. Micaelli, and A. Storkey, “Meta-learning in neural networks: A survey,” 2020.
- [20] A. Nichol, J. Achiam, and J. Schulman, “On first-order meta-learning algorithms,” *CoRR*, vol. abs/1803.02999, 2018. [Online]. Available: <http://arxiv.org/abs/1803.02999>
- [21] S. Liang, Y. Li, and R. Srikant, “Enhancing the reliability of out-of-distribution image detection in neural networks,” 2020.
- [22] Z. Ge, S. Demyanov, Z. Chen, and R. Garnavi, “Generative openmax for multi-class open set classification,” 2017.
- [23] L. Neal, M. Olson, X. Fern, W.-K. Wong, and F. Li, “Open set learning with counterfactual images,” in *Proceedings of the European Conference on Computer Vision (ECCV)*, September 2018.
- [24] Y. Chen, X. Wang, Z. Liu, H. Xu, and T. Darrell, “A new meta-baseline for few-shot learning,” *arXiv preprint arXiv:2003.04390*, 2020.
- [25] D. P. Kingma and M. Welling, “Auto-Encoding Variational Bayes,” in *2nd International Conference on Learning Representations, ICLR 2014, Banff, AB, Canada, April 14-16, 2014, Conference Track Proceedings*, 2014.
- [26] B. Dai, Y. Wang, J. Aston, G. Hua, and D. Wipf, “Connections with robust pca and the role of emergent sparsity in variational autoencoder models,” *The Journal of Machine Learning Research*, vol. 19, no. 1, pp. 1573–1614, 2018.
- [27] J. Liu, L. Song, and Y. Qin, “Prototype rectification for few-shot learning,” *ArXiv*, vol. abs/1911.10713, 2019.
- [28] S. Gidaris and N. Komodakis, “Dynamic few-shot visual learning without forgetting,” in *Proceedings of the IEEE Conference on Computer Vision and Pattern Recognition*, 2018, pp. 4367–4375.

- [29] N. Savinov, A. Raichuk, R. Marinier, D. Vincent, M. Pollefeys, T. Lillcrap, and S. Gelly, "Episodic curiosity through reachability," in *International Conference on Learning Representations (ICLR)*, 2019.
- [30] J. Stallkamp, M. Schlipsing, J. Salmen, and C. Igel, "Man vs. computer: Benchmarking machine learning algorithms for traffic sign recognition," *Neural networks : the official journal of the International Neural Network Society*, vol. 32, pp. 323–32, 02 2012.
- [31] Z. Zhu, D. Liang, S. Zhang, X. Huang, B. Li, and S. Hu, "Traffic-sign detection and classification in the wild," in *2016 IEEE Conference on Computer Vision and Pattern Recognition (CVPR)*, 2016, pp. 2110–2118.
- [32] A. Joly and O. Buisson, "Logo retrieval with a contrario visual query expansion," 01 2009, pp. 581–584.
- [33] P. Letessier, O. Buisson, and A. Joly, "Scalable mining of small visual objects," 10 2012.
- [34] S. Romberg, L. Pueyo, R. Lienhart, and R. Zwol, "Scalable logo recognition in real-world images," 01 2011, p. 25.
- [35] H. Su, X. Zhu, and S. Gong, "Deep learning logo detection with data expansion by synthesising context," *2017 IEEE Winter Conference on Applications of Computer Vision (WACV)*, pp. 530–539, 2017.
- [36] H.-Y. Tseng, H.-Y. Lee, J.-B. Huang, and M.-H. Yang, "Cross-domain few-shot classification via learned feature-wise transformation," *arXiv preprint arXiv:2001.08735*, 2020.
- [37] K. He, X. Zhang, S. Ren, and J. Sun, "Deep residual learning for image recognition," in *2016 IEEE Conference on Computer Vision and Pattern Recognition (CVPR)*, 2016, pp. 770–778.
- [38] D. P. Kingma and J. Ba, "Adam: A method for stochastic optimization," 2017.
- [39] L. van der Maaten and G. Hinton, "Visualizing data using t-sne," *Journal of Machine Learning Research*, vol. 9, no. 86, pp. 2579–2605, 2008. [Online]. Available: <http://jmlr.org/papers/v9/vandermaaten08a.html>
- [40] J. Deng, W. Dong, R. Socher, L. Li, Kai Li, and Li Fei-Fei, "Imagenet: A large-scale hierarchical image database," in *2009 IEEE Conference on Computer Vision and Pattern Recognition*, 2009, pp. 248–255.



Amit K. Roy-Chowdhury received his PhD from the University of Maryland, College Park (UMCP) in 2002 and joined the University of California, Riverside (UCR) in 2004 where he is a Professor and Bourns Family Faculty Fellow of Electrical and Computer Engineering, Director of the Center for Robotics and Intelligent Systems, and Cooperating Faculty in the department of Computer Science and Engineering. He leads the Video Computing Group at UCR, working on foundational principles of computer vision, image processing, and statistical learning, with applications in cyber-physical, autonomous and intelligent systems. He has published over 200 papers in peer-reviewed journals and conferences. He is the first author of the book *Camera Networks: The Acquisition and Analysis of Videos Over Wide Areas*. He is on the editorial boards of major journals and program committees of the main conferences in his area. His students have been first authors on multiple papers that received Best Paper Awards at major international conferences, including ICASSP and ICMR. He is a Fellow of the IEEE and IAPR, received the Doctoral Dissertation Advising/Mentoring Award 2019 from UCR, and the ECE Distinguished Alumni Award from UMCP.



Sayak Nag received his Bachelor's degree in Instrumentation and Electronics Engineering engineering from Jadavpur University, Kolkata, India. Currently, he is pursuing a Ph.D. in the Department of Electrical and Computer engineering at the University of California, Riverside. His broad research interests include computer vision and machine learning with a focus on few-shot learning, meta learning, open-set recognition and weakly-supervised learning.



Dripta S. Raychaudhuri received his Bachelor's degree in Electrical and Telecommunication engineering from Jadavpur University, Kolkata, India. Currently, he is pursuing a Ph.D. in the Department of Electrical and Computer engineering at the University of California, Riverside. His broad research interests include computer vision and machine learning with a focus on multi-task learning, domain adaptation and imitation learning.



Sujoy Paul is currently at Google Research. He received his PhD in Electrical and Computer Engineering from University of California, Riverside and his Bachelor's degree in Electronics and Telecommunication Engineering from Jadavpur University. His broad research interest includes Computer Vision and Machine Learning with more focus on semantic segmentation, human action recognition, domain adaptation, weak supervision, active learning, reinforcement learning, and so on.

APPENDIX A

DATASETS

In this section we go over the details of each dataset used in our experiments. A summary of the statistics of each dataset is shown in Table 7.

	GTSRB	TT100K	BelgaLogos	Flickr-32	TopLogos	miniImageNet
Number of Samples	51,839	11,988	9,585	3,404	848	60,000
Total Classes	43	36	37	32	11	100

TABLE 7: Number of samples and classes in each Dataset.

A.1 Traffic Sign Datasets.

GTSRB. This dataset [30] is one of the largest traffic-sign dataset. It is comprised of 43 classes broadly categorized under prohibitory, danger and mandatory categories. For GTSRB→GTSRB, the training set contains a total of 39,209 images and the test set has a total of 12,630 images. These images have variations in illumination, shading as well as, resolution [15].

TT100K. The Tsinghua-Tencent 100K (TT100K) [31] is a Chinese traffic sign detection dataset. This dataset has more than 200 categories, out of which we used the ones with valid annotation and a corresponding exemplar. Similar to [15] this amounts to a total of 36 valid classes to work with.

A.2 Brand Logo Datasets

BelgaLogos. BelgaLogos [32], [33] is comprised of 10,000 images of everyday brand logos commonly found in almost every aspect of daily life. The images have significant perturbations such as blurring, lighting and contrast variations as well as, occlusions. The dataset is also riddled with significant class imbalance as it contains classes with as little as 2 samples making it suitable for only 1-shot learning problems. Similar to [15] we collect 9,475 images from BelgaLogos categorised among 37 logo classes to construct our logo recognition dataset. The images of this dataset have a lot more variations compared to the traffic sign datasets, especially blurring and occlusion, which in-turn makes learning harder.

FlickrLogos-32. This dataset [34] is comprised of a collection of images corresponding to the 32 brand logos of Flickr. We use the splits introduced in [15], which is comprised of a total of 3,372 cropped logo images.

TopLogo-10. This dataset [35] contains logo images from 10 brands related to popular cloth, shoes and accessory brands. The logo images are obtained from their respective products and similar to [15] the collected images were cropped from bounding box annotations and divided among 11 classes where the ‘Adidas’ class is divided into ‘Adidas-logo’ and the ‘Adidas-text’.

A.3 Natural Image Dataset

miniImageNet. Originally proposed by Vinyals et. al. [11], *miniImageNet* has become a benchmark dataset for few-shot classification [9], [12]. It is derived from the larger ILSVRC-12 dataset [40] and is comprised of 100 classes each having 600 colored images, which are popularly resized to 84×84 [11], [12]. We use the same splits as [11] which comprises of a training set with 64 classes, a validation set with 16 classes and a test set with 20 classes.

APPENDIX B

TRAINING STRATEGY

For the traffic sign and brand logo classification, all modules of ReFOCS are trained end-to-end. However, for *miniImageNet* training the entire framework end-to-end results in over-powering of the reconstruction module resulting in decreased classification accuracy. We suspect, this problem is due to the difficult image-to-exemplar translation task for *miniImageNet* which is brought about by the fact that the exemplars of *miniImageNet* do not lie on a canonical domain, resulting in an embedding space where the seen class clusters have limited separation. In order to rectify this, we first meta-train the VAE encoder with just the cross-entropy classification loss (Eq. 6), following which the weights of trained encoder is fixed and utilized to jointly train the decoder and the novelty detection module using a combination of the reconstruction loss (Eq. 2) and the novelty detection loss (Eq. 8).

APPENDIX C

ABLATIONS

More ablation results are shown in tables 8 and 9. The details of each type ablation is provided in Section 4.4. Fig. 7 shows how the open-set AUROC is affected by the hyperparameters λ_1 or λ_3 for the GTSRB→TT100K task. In both cases, the classification term λ_2 is fixed at 10. In Fig. 7a, when λ_1 is very low, the open-set detection is hampered due to poor quality of the reconstruction and when it is increased beyond 10^{-4} reconstruction becomes the sole objective of the model, thus the open-set detection again degrades. From Fig. 7b we can see that for both the 5-shot and 1-shot cases increasing λ_3 causes the AUROC to improve the knee point of $\lambda_3 = 10$, after which it starts to degrade.

GTSRB→GTSRB				
EXPERIMENT	5-way 5-shot		5-way 1-shot	
	Acc.(%)	AUROC(%)	Acc.(%)	AUROC(%)
Recons. w/ AE	94.11 ± 0.37	94.61 ± 0.32	83.83 ± 0.79	91.81 ± 0.45
No modulation	93.11 ± 0.45	88.67 ± 0.55	84.34 ± 0.75	91.04 ± 0.54
ProtoC+ND	89.72 ± 0.56	82.23 ± 0.79	82.79 ± 0.78	77.56 ± 0.92
No embedding	93.55 ± 0.41	88.80 ± 0.61	85.78 ± 0.72	88.62 ± 0.61
No clf	94.09 ± 0.35	94.03 ± 0.34	84.62 ± 0.78	92.10 ± 0.43
ReFOCS (Ours)	94.17 ± 0.38	94.83 ± 0.35	86.21 ± 0.78	93.02 ± 0.45

GTSRB→TT100K				
EXPERIMENT	5-way 5-shot		5-way 1-shot	
	Acc.(%)	AUROC(%)	Acc.(%)	AUROC(%)
Recons. w/ AE	81.33 ± 0.80	77.08 ± 0.79	68.59 ± 0.88	75.71 ± 0.71
No modulation	80.94 ± 0.79	78.55 ± 0.65	69.84 ± 0.91	77.75 ± 0.54
ProtoC+ND	76.92 ± 0.83	72.50 ± 0.61	68.59 ± 0.83	71.61 ± 0.76
No embedding	83.03 ± 0.75	74.33 ± 0.66	70.77 ± 0.87	59.28 ± 0.79
No clf	82.71 ± 0.74	82.85 ± 0.56	69.14 ± 0.94	74.63 ± 0.61
ReFOCS (Ours)	83.36 ± 0.76	85.25 ± 0.56	71.45 ± 0.87	81.98 ± 0.59

TABLE 8: **Ablation studies on traffic sign recognition.** Recons. w/ AE refers to swapping the VAE with an Autoencoder (AE); No Modulation denotes turning off embedding modulation; No embedding/clf denote the removal of embedding/softmax scores from the input of the novelty module. ProtoC+ND refers to when we donot use exemplars for the reconstruction and consequently, remove the reconstruction errors from the input of the novelty module.

EXPERIMENT	BELGA→FLICKR32		BELGA→TOPLOGOS	
	5-way 1-shot		5-way 1-shot	
	Acc.(%)	AUROC(%)	Acc.(%)	AUROC(%)
Recons. w/ AE	63.13 ± 1.05	71.86 ± 0.86	36.40 ± 2.00	56.37 ± 1.95
No modulation	63.26 ± 1.03	56.69 ± 0.97	41.75 ± 1.99	52.83 ± 1.93
ProtoC+ND	61.64 ± 1.03	50.01 ± 0.99	41.60 ± 2.04	50.52 ± 2.06
No embedding	65.49 ± 1.00	67.79 ± 0.91	41.45 ± 2.01	53.52 ± 2.11
No clf	64.51 ± 1.01	71.58 ± 0.87	38.60 ± 1.96	56.62 ± 1.86
ReFOCS (Ours)	66.29 ± 1.02	72.98 ± 0.83	42.30 ± 2.15	58.39 ± 1.97

TABLE 9: **Ablation studies on brand logo recognition.** Recons. w/ AE refers to swapping the VAE with an Autoencoder (AE); No Modulation denotes turning off embedding modulation; No embedding/clf denote the removal of embedding/softmax scores from the input of the novelty module. ProtoC+ND refers to when we donot use exemplars for the reconstruction and consequently, remove the reconstruction errors from the input of the novelty module.

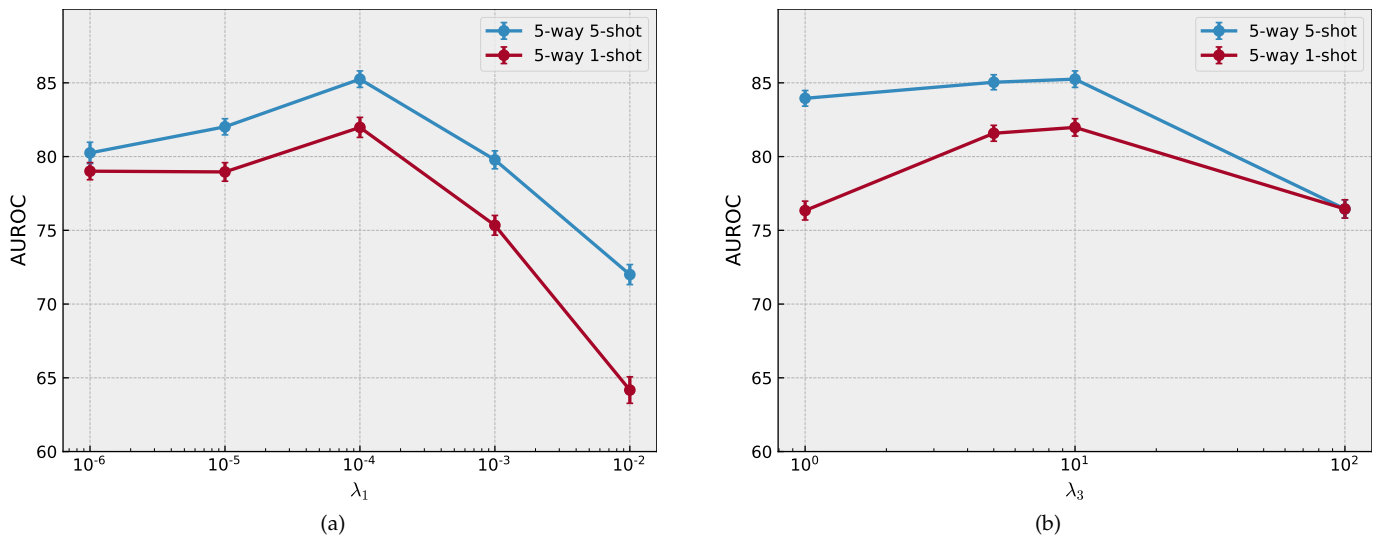


Fig. 7: **Hyperparameter Analysis.** (a) λ_2 & λ_3 are fixed at 5 and 10, changing only the reconstruction loss term. (b) λ_1 and λ_2 are fixed at 10^{-4} and 10 and λ_3 is varied.